

UCLA

UCLA Previously Published Works

Title

Cardiovascular MRI with ferumoxytol

Permalink

<https://escholarship.org/uc/item/62d9n3wn>

Journal

Clinical Radiology, 71(8)

ISSN

0009-9260

Authors

Finn, JP
Nguyen, K-L
Han, F
[et al.](#)

Publication Date

2016-08-01

DOI

10.1016/j.crad.2016.03.020

Peer reviewed



Published in final edited form as:

Clin Radiol. 2016 August ; 71(8): 796–806. doi:10.1016/j.crad.2016.03.020.

Cardiovascular MR Imaging with Ferumoxytol

J. Paul Finn, MD^{1,2}, Kim-Lien Nguyen^{1,3}, Fei Han^{1,2}, Ziwu Zhou^{1,2}, Isidro Salusky^{1,5}, Ihab Ayad^{1,4}, Peng Hu^{1,2}

¹Diagnostic Cardiovascular Imaging Laboratory, David Geffen School of Medicine at UCLA, Los Angeles, CA

²Department of Radiological Sciences, David Geffen School of Medicine at UCLA, Los Angeles, CA

³Division of Cardiology, David Geffen School of Medicine at UCLA and VA Greater Los Angeles Healthcare System, Los Angeles, CA

⁴Department of Anesthesiology, David Geffen School of Medicine at UCLA, Los Angeles, CA

⁵Division of Pediatric Nephrology, David Geffen School of Medicine at UCLA, Los Angeles, CA

Abstract

The practice of contrast enhanced magnetic resonance angiography (CEMRA) has changed significantly in the span of a decade. Concerns regarding gadolinium (Gd)-associated nephrogenic systemic fibrosis in those with severely impaired renal function spurred developments in low-dose CEMRA and non-contrast MRA as well as efforts to seek alternative MR contrast agents. Originally developed for MRI use, ferumoxytol (an ultra-small superparamagnetic iron oxide nanoparticle), is currently approved by the United States (U.S.) Food and Drug Administration for the treatment of iron deficiency anemia in adults with renal disease. Since its clinical availability in 2009, there has been rising interest in the scientific and clinical use of ferumoxytol as an MR contrast agent. The unique physicochemical and pharmacokinetic properties of ferumoxytol, including its long intravascular half-life and high r_1 relaxivity, support a spectrum of MRI applications beyond the scope of Gd-based contrast agents. Moreover, whereas Gd is not found in biological systems, iron is essential for normal metabolism, and nutritional iron deficiency poses major public health challenges worldwide. Once the carbohydrate shell of ferumoxytol is degraded, the elemental iron at its core is incorporated into the reticuloendothelial system. These considerations position ferumoxytol as a potential game changer in the field of CEMRA and MRI. In this paper, we aim to summarize our experience on the cardiovascular applications of ferumoxytol and provide a brief synopsis of ongoing investigations on ferumoxytol-enhanced MR applications.

Corresponding author and reprint info: J. Paul Finn, MD, Department of Radiological Sciences, University of California at Los Angeles, Peter V. Ueberroth Building Suite 3371, 10945 Le Conte Ave., Los Angeles, CA 90095-7206, USA, Phone: 310.825.0958, Fax: 310.825.0880, pfinn@mednet.ucla.edu.

Author contributions: Guarantor of integrity of the entire study (JPF, PH, KLN). Study concepts and design (JPF, PH, KLN). Literature search (JPF, PH, KLN). Clinical studies (JPF, IA). Experimental studies/data analysis (N/A). Statistical analysis (N/A). Manuscript preparation (JPF, PH, KLN, FH, ZZ). Manuscript editing (all authors).

Disclosures: None

Introduction

A decade ago, the second most common indication for Gadolinium (Gd) use was contrast enhanced MR angiography (CEMRA). CT had become unfashionable and the only remaining outpost for non-contrast MRA was the cranium. To boot, double or triple dose Gd was the rule and there were no safety concerns in renal impairment. In fact, renal failure was an *indication* for gadolinium. The landscape changed dramatically when Gd was implicated in the causation of nephrogenic systemic fibrosis (NSF) (1) and high dose CEMRA was singled out as the main perpetrator (2). The response of the MR community was swift, decisive and remarkably effective (3). Within a few years, NSF was virtually eradicated, providing tacit evidence, if not outright proof, that Gd had been the culprit. Administration of gadolinium based contrast agents (GBCA) has since ceased to be routine and pre-testing of renal function has assumed a role not dissimilar to that for X-ray contrast media (4). Other than in exceptional circumstances, severe renal impairment now contraindicates the use of GBCA and even milder forms of renal impairment make many clinicians reluctant to order contrast MRI. The practice of CEMRA has been changed profoundly.

Not surprisingly, there has been a resurgence of interest in non-contrast (NC) MRA techniques, spurring new developments and innovations (5–12). In parallel, the pharmaceutical industry and academic practitioners have sought to manage risk while maintaining functionality with CEMRA. Specific formulations of GBCA have been touted as safer and more stable than others (13–15) and low dose GBCA protocols have been established (16–19). Recognizing the likely lower risk with some GBCAs than others, in September 2010, the United States Food and Drug Administration (FDA) updated their warning to classify the GBCA based on their relative risk in patients with renal failure and advising low dose protocols where possible (20).

Today, the field is in flux, with NC-MRA techniques undergoing evaluation and low dose CEMRA protocols becoming standard. However, in the nine years or so since NSF was first recognized, the community remains sensitive to NSF and clinical practice has adapted to the new reality.

Non-gadolinium contrast agents are not widely used for MRI. Of these, the best known is ferumoxides (Feridex[®], Bayer-Schering Pharmaceuticals), a colloidal iron suspension used for imaging the liver and reticuloendothelial system (RES) (21). Ferumoxides were administered by slow intravenous infusion and in clinical trials were associated with allergic or anaphylactic reactions in 0.5% and with back pain in up to 2% of patients (22). Although ferumoxides are effective agents for imaging the liver and RES, their mode of action is predominantly shortening of T2 and they are not suitable agents for CEMRA. Today, they have been largely superseded by gadoxetate (Eovist[®], Bayer Schering Pharm), a hepatocyte specific GBCA, which also attracts the FDA boxed warning about NSF risk.

Of the iron-based agents, ferumoxytol has generated the most excitement and promise for cardiovascular imaging and has recently emerged from obscurity as a potential diamond in the rough. Ferumoxytol (Feraheme[®], AMAG Pharmaceuticals, Waltham, MA, U.S.; Rienso[®], Takeda Pharmaceuticals, London, UK) is an iron-based nanoparticle with a mean

diameter of 30 nm and is a member of the class of ultra-small, superparamagnetic iron oxide (USPIO) particles, originally designed as an intravascular contrast agent for MRI. Its iron oxide core is embedded in a dextran coat, which diminishes immunogenicity and retards phagocytosis and the release of elemental iron from the core. As a result, ferumoxytol has a long intravascular half-life of about 15 hours and is taken up only slowly by the macrophages of the RES. Importantly, ferumoxytol has a high R1 relaxivity ($r_1 \sim 15 \text{ mM}^{-1}\text{s}^{-1}$ at 1.5T) such that it can be used for bright blood imaging. Ferumoxytol-enhanced MRA was first described in 1997 by Anzai et al (23) and later in a clinical pilot study by Prince et al (24). An initial clinical comparison with gadopentetate dimeglumine for CEMRA by Li et al in 2005 (25) suggested near equivalence for both agents and the company did not seek an imaging indication. Instead, ferumoxytol underwent clinical trials as a rapid injection agent for treatment of iron deficiency anemia in adults with chronic kidney disease and was approved by the U.S. FDA in 2009 as Feraheme[®]. Little further was reported in the literature about ferumoxytol for CEMRA until the papers by Sigovan et al. in 2012 (26) and Bashir et al. in 2013 (27), addressing the use of ferumoxytol in patients with severe renal disease. In 2015, the first reports of ferumoxytol for CEMRA in children were published by Nayak et al (28), Han et al (29) and Ruangwattanapaisarn et al (30). All of these recent studies reported outstanding results with no serious adverse events (SAE) and few if any minor adverse events (AE).

Within the past three years, several groups have explored the use of ferumoxytol for cardiovascular MRI (25, 31–33). Recent works (28–30) highlighted its use for vascular and cardiac imaging in the pediatric population. In this paper, we explore some of the potential clinical applications of ferumoxytol in adults and children, pointing out differences and similarities between its use and that of the gadolinium based agents. We will draw largely from our own experience as well as from that of the limited number of centers, which have used the agent for broad or specific indications. All of the patient studies described in this paper were performed with written informed consent from the patients or their legal guardians and with the approval of our institutional review board (IRB).

Pharmacokinetics and technique

At this point, it may be useful to review some of the relevant properties of ferumoxytol (48), within the context of the more traditional GBCAs. Ferumoxytol shares several attributes found within the class of GBCA, but it possesses a combination of properties, which may support a new paradigm for vascular imaging. First, because of its size, ferumoxytol is impermeable to vascular capillaries and is not filtered by the kidneys. It therefore remains in the blood until phagocytized by the macrophages of the reticuloendothelial system (RES). However, unlike the ferumoxides, which are cleared from the blood by the RES within minutes, ferumoxytol is taken up slowly and has a blood half-life of about 15 hours (48). In the context of a diagnostic imaging study, this guarantees a constant blood concentration once the steady state distribution is achieved. For practical purposes, this steady state distribution will be established within 2–3 minutes of injection in everybody. Second, ferumoxytol has an r_1 relaxivity of $15 \text{ mM}^{-1} \text{ s}^{-1}$ at 1.5T (48). This value is similar to that of gadofosveset (Ablavar[®], Lantheus Medical Imaging) which, among the GBCA group, most closely resembles ferumoxytol in terms of potency and vascular residence time. However,

whereas ferumoxytol is a pure intravascular agent, gadofosveset binds reversibly to serum albumin, such that at any time upwards of 20% is present in the blood as free Gd-DTPA. The unbound moiety diffuses into the interstitial space with a half-life of about 30 minutes and is filtered by the kidneys, which are the route of elimination. For this reason, the blood concentration of gadofosveset starts to decline once its steady state distribution is achieved, albeit at a slower rate than the pure extracellular GBCAs. Third, ferumoxytol has a strong T2 relaxivity ($89 \text{ mM}^{-1} \text{ s}^{-1}$ at 1.5T). Therefore, with appropriate pulse sequences, fully reliable black blood imaging becomes trivial. These properties of ferumoxytol can be exploited to increase the simplicity, reliability and versatility of vascular imaging. Sample technical parameters for FEMRA are outlined in Table 1.

Overview of Clinical Applications for Ferumoxytol enhanced MRA (FEMRA).

The majority of publications on FEMRA focus on patients with renal failure (Table 2), where GBCAs are relatively contraindicated. The paper by Sigovan et al (26) addressed the patency of dialysis fistulae and paved the way for the more widespread use of ferumoxytol for imaging renal transplants (27) and pelvic veins (43). These authors also speculated appropriately on the broader potential of ferumoxytol as a vascular imaging agent.

From July 2013 to March 2015, we performed first pass and steady state FEMRA in children who needed vascular mapping for venous access, organ transplant workup or to assess the status of renal transplants. In due course, we expanded the target population to include adults with renal failure and children with congenital heart disease. Our default field strength for CEMRA and FEMRA is 3.0T and we routinely use anesthesia with controlled ventilation for children under 6 years of age and for older children who are unable to cooperate for any reason. Based on earlier published results at 1.5T (25), we initially used a dose of 4 mg/kg for first pass and steady state FEMRA, but settled on 2 mg/kg for first pass, supplemented to a total dose of 4 mg/kg for steady state FEMRA at 3.0T. This became our standard protocol for children and adults. However, since the FDA black box warning in March 2015, cautioning against bolus injection of ferumoxytol, we have replaced our first pass FEMRA protocols with steady state FEMRA only. We now administer dilute ferumoxytol by slow intravenous infusion over 10 minutes, with continuous monitoring of blood pressure and heart rate. In our experience, for most clinical applications in the chest, abdomen and pelvis, first pass imaging is dispensable. As illustrated below, detailed vascular imaging can be performed with ferumoxytol in the steady state, and in many cases the process of image acquisition is greatly simplified whereas image post-processing assumes a more central role.

Aortic imaging

For most applications, the aorta and its major branches can be imaged reliably with ferumoxytol either on first pass (Fig 1 A,C) or in steady state. For detection of atheromatous narrowing, tortuosity or aneurysm, there seems little disadvantage to performing only steady state imaging (Fig 1 B,D,E). A dearth of clinical data exist on the use of ferumoxytol in acute or chronic dissection, but it seems intuitive that information about the sequence of filling of true and false lumens, such as is available from a time-resolved acquisition, would be desirable. However, although first pass imaging can highlight differential rates

of enhancement in true and false lumens (Fig 2A,B), the overall anatomy may be fully represented in the steady state images (Fig 2C). Because of the high signal gradient between lumen and wall, image segmentation of the vascular space into its components is a simpler task with ferumoxytol than with the extracellular agents. Also, whereas confusion between slow flow and mural or intraluminal thrombus can plague conventional black blood imaging techniques, with ferumoxytol this becomes a moot point (Fig 3). On spin echo techniques such as HASTE, with even a modest TE (on the order of 30 ms), the signal from blood decays without the need for magnetization preparation pulses. The implications of this effect are significant both for immediate clinical practice and for future work on plaque imaging.

Transcatheter Aortic Valve Replacement (TAVR).

Patients being considered for TAVR are typically elderly with a high prevalence of renal impairment. Further, deterioration in renal function complicating the TAVR procedure is one of the major determinants of post procedural morbidity and mortality (49–53). Whereas CTA is widely regarded as the current standard for pre-procedural mapping of arterial access anatomy prior to TAVR, cumulative doses of iodinated contrast prior to and during the procedure can predispose to contrast nephropathy (54, 55). For this reason, our cardiologists have chosen ferumoxytol MRI over CTA for arterial access mapping in TAVR candidates with renal impairment. We have used ferumoxytol equally successfully with first pass (Fig 1A,C) and steady state imaging (Fig 1B, D, E and Fig 4A) to image the access vessels from the groin to the aortic annulus. Further, the steady state distribution of ferumoxytol supports high quality spoiled gradient echo cine imaging, even at 3.0T, and these can be used to supplement dynamic information about transvalvar pressure gradients, planimetered areas, coronary ostia and leaflet motility (Fig 4B).

Venographic Imaging

Ferumoxytol enhances the entire blood pool in a stable and specific way and this is a powerful attribute for a venographic imaging agent. Children and adults with organ failure may require venous imaging for line placement, pre- or post-transplant evaluation or suspected thrombosis. The frequent occurrence of renal impairment in these patients complicates the use of iodinated contrast and GBCAs, and unpredictable flow patterns can pose a challenge for non-contrast MRA. Furthermore, even though CT can generate superb spatial resolution with ever increasing speed, the quality of venous imaging is fundamentally determined by the contrast enhancement status of the blood pool. In steady state, CT contrast agents become greatly diluted and image quality suffers. With ferumoxytol, once distributed in the blood pool, little change occurs for several hours, either from redistribution or elimination. Venous imaging becomes as simple as injection and steady state acquisition, with breath holding as required. Also, in the steady state, multiple overlapping stations can be acquired in separate breath holds and composed into a single large field of view image, without concerns about differential regional vascular enhancement. Figure 5 illustrates these points in a striking example of CT venography and ferumoxytol venography in the same patient. Moreover, because bolus timing is not an issue, if breathing motion artifact occurs when imaging the chest or abdomen, the acquisition can be repeated as needed and imaging parameters adjusted as required.

Congenital heart disease

Children with complex congenital heart disease (CHD) present a unique challenge for MRI and some of the more intriguing applications of ferumoxytol may be in this group. MRI has long been recognized as a powerful modality both in children and adults with CHD and 1.5T has long remained the favored field strength for cardiac MRI. Our experience and that of others suggests that ferumoxytol may shift the focus towards 3.0T for patients with CHD. In most specialized centers, cardiac MRI in patients younger than 6 years is performed under anesthesia with controlled ventilation (56). Under these circumstances, strategies for physiological motion correction can be very successful and data acquisition windows which span several minutes can generate both highly temporally and highly spatially resolved images. In the past, researchers have generated 4D bSSFP (balanced steady state free precession) images, or '3D cine' of the beating heart (57–59) without the need for contrast enhancement. However, image quality with bSSFP cine at 3.0T has been unreliable due to off-resonance artifact and RF non-uniformity and this has impeded the more widespread adoption of 3.0T for cardiac MRI. With ferumoxytol in the steady state, the short and stable T1 of the blood can be exploited by the use of high bandwidth 3D, spoiled gradient echo techniques which, when compared to bSSFP, are practically immune to off-resonance artifact and RF non-uniformity. Also, with physiologic motion correction, multiple 3D phases with isotropic spatial resolution can be acquired over the cardiac cycle. Recently, our group implemented such a technique, called MUSIC (Multiphase Steady state Imaging with Contrast), during the steady state distribution phase of ferumoxytol in children (29), while Cheng et al have applied a similar approach to 4D flow imaging (60).

In patients whose cardiac and respiratory rhythms are regular over several minutes, physiological motion correction strategies have proved highly effective. Ferumoxytol provides a stable blood pool signal resistant to saturation, such that very short repetition times and echo times can be used to minimize acquisition time and optimize image quality. In our experience, the efficiency of ventilator gating ranges from 45% to 65%, without specific maneuvers to modify the respiratory waveform. 4D data with sub-millimeter resolution are typically acquired in 7–10 minutes during uninterrupted mechanical ventilation. Fig 6 shows MUSIC images in a 19-month-old male with stridor due to a double aortic arch. Complete evaluation of cardiac and vascular anatomy was provided by a single 8-minute 4D acquisition during continuous ventilation. Further, because the data are spatially isotropic and time-resolved, they can be reformatted into 2D cine slices of arbitrary orientation and thickness and can serve as surrogates for conventional 2D breath held cine. Accelerated and improved extensions of MUSIC are under development in our laboratory, including compressed sensing (61) and self-gated (62) versions. Further work remains to be done to validate the techniques against conventional clinical MRI standards.

The approach of acquiring non-breath-held, high-resolution 4D datasets stands to define a new paradigm, potentially replacing the current practice of repeated breath, multi-slice cine and 3D angiography. If validated, the 4D approach may greatly simplify and accelerate the process of image acquisition and make moot the requirement for a specialized CHD physician to be present guiding the scan. The emphasis then shifts from prospective image

acquisition to post-acquisition image processing and reformatting, generating potentially limitless imaging planes for interrogation at any time in the future.

Safety profile

Interest in the diagnostic use of ferumoxytol was growing rapidly until March 2015, when the U.S. FDA issued a Black Box Warning highlighting post-marketing surveillance reports of SAE in 79 adult CKD patients who received ferumoxytol injection for treatment of iron deficient anemia and of whom 18 died. Within this time frame, more approximately 1.2 million vials of Feraheme[®] were sold (personal communication from the manufacturer in September 2015). In three pre-marketing clinical trials of Feraheme[®], which encompassed 1,164 patients (34–36), the aggregate rate of anaphylaxis was approximately 0.2% and this is the rate specified in the package insert. The largest post-marketing clinical trial for therapeutic use of Feraheme[®] (37) encompassed 8,666 patients with CKD and noted a SAE rate of 0.2% (18/8,666) and an anaphylaxis rate of 0.02% (2/8,666). In Europe, ferumoxytol was approved by the European Commission in June of 2012 as Rienso[®] following positive opinions by the European Medicines Agency (38). However, as a request from Takeda Pharmaceuticals, Rienso[®] was withdrawn from European markets in July 2015 (39).

Within the past decade, there have been a number of studies describing the diagnostic use of ferumoxytol for both adults and children (25, 27, 28, 30, 32, 40–47) with approximately 300 patients and no SAE was reported. Whereas details of the circumstances surrounding the 79 SAE referenced in the FDA warning are not yet widely available, limited data reviewed by the authors suggest that most cases were confounded by multiple co-morbidities. Nonetheless, although at the time of writing we are unaware of any cases of anaphylaxis surrounding the diagnostic use of ferumoxytol, pending more extensive safety data and analysis, ferumoxytol should be considered for diagnostic use only when there is a strong clinical indication with a prospect of direct benefit to the patient and with appropriate physiological monitoring.

Summary

Within the past three years, there have been rapid advances and challenging delays in the application of ferumoxytol for MRI of the cardiovascular system. Among scientists and clinicians who have used ferumoxytol, there is widespread enthusiasm and consensus about its performance and potential. However, at the time of this writing, the main obstacles to further development center around safety concerns relating to the risk of severe allergic reactions following intravenous injection. Whereas the published safety data from clinical trials are highly encouraging and suggest a low incidence of anaphylactoid type occurrences, recent statements from the FDA have put the imaging community on alert and more extensive clinical trials addressing the safety and effectiveness of ferumoxytol as an MRI contrast agent are warranted and will be eagerly anticipated.

Funding sources:

This work is supported by grant R01HL127153 from the National Heart, Lung, and Blood Institute.

References

1. Kuo PH, Kanal E, Abu-Alfa AK, Cowper SE. Gadolinium-based MR contrast agents and nephrogenic systemic fibrosis. *Radiology*. 2007;242(3):647–649. [PubMed: 17213364]
2. Deo A, Fogel M, Cowper SE. Nephrogenic systemic fibrosis: a population study examining the relationship of disease development to gadolinium exposure. *Clinical journal of the American Society of Nephrology : CJASN*. 2007;2(2):264–267. [PubMed: 17699423]
3. Kanal E, Barkovich AJ, Bell C, et al. ACR guidance document for safe MR practices: 2007. *AJR American journal of roentgenology*. 2007;188(6):1447–1474. [PubMed: 17515363]
4. American College of Radiology. ACR Manual on Contrast Media (Version 10). 2015. Accessed September 1, 2015. 79–93. <http://www.acr.org/~media/37D84428BF1D4E1B9A3A2918DA9E27A3.pdf>.
5. Edelman RR, Sheehan JJ, Dunkle E, Schindler N, Carr J, Koktzoglou I. Quiescent-interval single-shot unenhanced magnetic resonance angiography of peripheral vascular disease: Technical considerations and clinical feasibility. *Magnetic resonance in medicine : official journal of the Society of Magnetic*. 2010;63(4):951–958.
6. Miyazaki M, Sugiura S, Tateishi F, Wada H, Kassai Y, Abe H. Non-contrast-enhanced MR angiography using 3D ECG-synchronized half-Fourier fast spin echo. *J Magn Reson Imaging*. 2000;12(5):776–783. [PubMed: 11050650]
7. Brittain JH, Olcott EW, Szuba A, et al. Three-dimensional flow-independent peripheral angiography. *Magnetic resonance in medicine : official journal of the Society of Magnetic*. 1997;38(3):343–354.
8. Katoh M, Buecker A, Stuber M, Gunther RW, Spuentrup E. Free-breathing renal MR angiography with steady-state free-precession (SSFP) and slab-selective spin inversion: initial results. *Kidney international*. 2004;66(3):1272–1278. [PubMed: 15327427]
9. Priest AN, Graves MJ, Lomas DJ. Non-contrast-enhanced vascular magnetic resonance imaging using flow-dependent preparation with subtraction. *Magnetic resonance in medicine : official journal of the Society of Magnetic*. 2012;67(3):628–637.
10. Fan Z, Sheehan J, Bi X, Liu X, Carr J, Li D. 3D noncontrast MR angiography of the distal lower extremities using flow-sensitive dephasing (FSD)-prepared balanced SSFP. *Magnetic resonance in medicine : official journal of the Society of Magnetic*. 2009;62(6):1523–1532.
11. Hodnett PA, Ward EV, Davarpanah AH, et al. Peripheral arterial disease in a symptomatic diabetic population: prospective comparison of rapid unenhanced MR angiography (MRA) with contrast-enhanced MRA. *AJR American journal of roentgenology*. 2011;197(6):1466–1473. [PubMed: 22109304]
12. Kwon KT, Kerr AB, Wu HH, Hu BS, Brittain JH, Nishimura DG. Non-contrast-enhanced peripheral angiography using a sliding interleaved cylinder acquisition. *Magnetic resonance in medicine : official journal of the Society of Magnetic*. 2015;74(3):727–738.
13. Prince MR, Zhang H, Zou Z, Staron RB, Brill PW. Incidence of immediate gadolinium contrast media reactions. *AJR American journal of roentgenology*. 2011;196(2):W138–143. [PubMed: 21257854]
14. Raisch DW, Garg V, Arabyat R, et al. Anaphylaxis associated with gadolinium-based contrast agents: data from the Food and Drug Administration’s Adverse Event Reporting System and review of case reports in the literature. *Expert opinion on drug safety*. 2014;13(1):15–23. [PubMed: 24053773]
15. Aran S, Shaqdan KW, Abujudeh HH. Adverse allergic reactions to linear ionic gadolinium-based contrast agents: experience with 194, 400 injections. *Clin Radiol*. 2015;70(5):466–475. [PubMed: 25626627]
16. Tomasian A, Salamon N, Lohan DG, Jalili M, Villablanca JP, Finn JP. Supraaortic arteries: contrast material dose reduction at 3.0-T high-spatial-resolution MR angiography--feasibility study. *Radiology*. 2008;249(3):980–990. [PubMed: 19011192]
17. Habibi R, Krishnam MS, Lohan DG, et al. High-spatial-resolution lower extremity MR angiography at 3.0 T: contrast agent dose comparison study. *Radiology*. 2008;248(2):680–692. [PubMed: 18574136]

18. Nael K, Krishnam M, Nael A, Ton A, Ruehm SG, Finn JP. Peripheral contrast-enhanced MR angiography at 3.0T, improved spatial resolution and low dose contrast: initial clinical experience. *Eur Radiol.* 2008;18(12):2893–2900. [PubMed: 18618122]
19. Wang J, Yan F, Liu J, et al. Multicenter, intra-individual comparison of single dose gadobenate dimeglumine and double dose gadopentetate dimeglumine for MR angiography of the peripheral arteries (the Peripheral VALUE Study). *J Magn Reson Imaging.* 2013;38(4):926–937. [PubMed: 23371919]
20. US Food and Drug Administration. FDA Drug Safety Communication: New warnings for using gadolinium-based contrast agents in patients with kidney dysfunction. 2010. Accessed January 27, 2016. <http://www.fda.gov/Drugs/DrugSafety/ucm223966.htm>.
21. Ros PR, Freeny PC, Harms SE, et al. Hepatic MR imaging with ferumoxides: a multicenter clinical trial of the safety and efficacy in the detection of focal hepatic lesions. *Radiology.* 1995;196(2):481–488. [PubMed: 7617864]
22. Bayer. Feridex Drug Label. 2007.
23. Anzai Y, Prince MR, Chenevert TL, et al. MR angiography with an ultrasmall superparamagnetic iron oxide blood pool agent. *J Magn Reson Imaging.* 1997;7(1):209–214. [PubMed: 9039617]
24. Prince MR, Zhang HL, Chabra SG, Jacobs P, Wang Y. A pilot investigation of new superparamagnetic iron oxide (ferumoxytol) as a contrast agent for cardiovascular MRI. *Journal of X-ray science and technology.* 2003;11(4):231–240. [PubMed: 22388293]
25. Li W, Tutton S, Vu AT, et al. First-pass contrast-enhanced magnetic resonance angiography in humans using ferumoxytol, a novel ultrasmall superparamagnetic iron oxide (USPIO)-based blood pool agent. *J Magn Reson Imaging.* 2005;21(1):46–52. [PubMed: 15611942]
26. Sigovan M, Gasper W, Alley HF, Owens CD, Saloner D. USPIO-enhanced MR angiography of arteriovenous fistulas in patients with renal failure. *Radiology.* 2012;265(2):584–590. [PubMed: 22875796]
27. Bashir MR, Jaffe TA, Brennan TV, Patel UD, Ellis MJ. Renal transplant imaging using magnetic resonance angiography with a nonnephrotoxic contrast agent. *Transplantation.* 2013;96(1):91–96. [PubMed: 23680931]
28. Nayak AB, Luhar A, Hanudel M, et al. High-resolution, whole-body vascular imaging with ferumoxytol as an alternative to gadolinium agents in a pediatric chronic kidney disease cohort. *Pediatric nephrology (Berlin, Germany).* 2015;30(3):515–521. [PubMed: 25212105]
29. Han F, Rapacchi S, Khan S, et al. Four-dimensional, multiphase, steady-state imaging with contrast enhancement (MUSIC) in the heart: A feasibility study in children. *Magnetic resonance in medicine : official journal of the Society of Magnetic.* 2015 Oct;74(4):1042–1049.
30. Ruangwattanapaisarn N, Hsiao A, Vasanawala SS. Ferumoxytol as an off-label contrast agent in body 3T MR angiography: a pilot study in children. *Pediatr Radiol.* 2015 Jun;45(6):831–839. [PubMed: 25427433]
31. Bashir MR, Bhatti L, Marin D, Nelson RC. Emerging applications for ferumoxytol as a contrast agent in MRI. *J Magn Reson Imaging.* 2015 Apr;41(4):884–898. [PubMed: 24974785]
32. Walker JP, Nosova E, Sigovan M, et al. Ferumoxytol-Enhanced Magnetic Resonance Angiography is a Feasible Method for the Clinical Evaluation of Lower Extremity Arterial Disease. *Annals of vascular surgery.* 2015;29(1):63–68. [PubMed: 25269682]
33. Yilmaz A, Rosch S, Yildiz H, Klumpp S, Sechtem U. First multiparametric cardiovascular magnetic resonance study using ultrasmall superparamagnetic iron oxide nanoparticles in a patient with acute myocardial infarction: new vistas for the clinical application of ultrasmall superparamagnetic iron oxide. *Circulation.* 2012;126(15):1932–1934. [PubMed: 23044610]
34. Spinowitz BS, Kausz AT, Baptista J, et al. Ferumoxytol for treating iron deficiency anemia in CKD. *J Am Soc Nephrol.* 2008;19(8):1599–1605. [PubMed: 18525001]
35. Singh A, Patel T, Hertel J, Bernardo M, Kausz A, Brenner L. Safety of ferumoxytol in patients with anemia and CKD. *Am J Kidney Dis.* 2008;52(5):907–915. [PubMed: 18824288]
36. Provenzano R, Schiller B, Rao M, Coyne D, Brenner L, Pereira BJ. Ferumoxytol as an intravenous iron replacement therapy in hemodialysis patients. *Clinical journal of the American Society of Nephrology : CJASN.* 2009;4(2):386–393. [PubMed: 19176796]

37. Schiller B, Bhat P, Sharma A. Safety and effectiveness of ferumoxytol in hemodialysis patients at 3 dialysis chains in the United States over a 12-month period. *Clinical therapeutics*. 2014;36(1):70–83. [PubMed: 24315802]
38. Takeda. Rienso. 2012. Accessed January 23, 2016. https://www.takeda.com/news/2012/20120625_3975.html.
39. European Medicines Agency. Rienso. 2015. Accessed January 23, 2016. http://www.ema.europa.eu/ema/index.jsp?curl=pages/medicines/human/medicines/002215/human_med_001569.jsp&mid=WC0b01ac058001d124.
40. Ning P, Zucker EJ, Wong P, Vasanaawala SS. Hemodynamic safety and efficacy of ferumoxytol as an intravenous contrast agents in pediatric patients and young adults. *Magnetic resonance imaging*. 2016;34(2):152–158. [PubMed: 26518061]
41. Muehe AM, Feng D, von Eyben R, et al. Safety Report of Ferumoxytol for Magnetic Resonance Imaging in Children and Young Adults. *Invest Radiol*. 2015.
42. Klenk C, Gawande R, Uslu L, et al. Ionising radiation-free whole-body MRI versus (18)F-fluorodeoxyglucose PET/CT scans for children and young adults with cancer: a prospective, non-randomised, single-centre study. *The Lancet Oncology*. 2014;15(3):275–285. [PubMed: 24559803]
43. Bashir MR, Mody R, Neville A, et al. Retrospective assessment of the utility of an iron-based agent for contrast-enhanced magnetic resonance venography in patients with endstage renal diseases. *J Magn Reson Imaging*. 2014;40(1):113–118. [PubMed: 24130008]
44. Alam SR, Shah AS, Richards J, et al. Ultrasmall superparamagnetic particles of iron oxide in patients with acute myocardial infarction: early clinical experience. *Circulation Cardiovascular imaging*. 2012;5(5):559–565. [PubMed: 22875883]
45. Thompson EM, Guillaume DJ, Dosa E, et al. Dual contrast perfusion MRI in a single imaging session for assessment of pediatric brain tumors. *Journal of neuro-oncology*. 2012;109(1):105–114. [PubMed: 22528798]
46. Hassan N, Cahill J, Rajasekaran S, Kovey K. Ferumoxytol infusion in pediatric patients with gastrointestinal disorders: first case series. *The Annals of pharmacotherapy*. 2011;45(12):e63. [PubMed: 22116997]
47. D’Arceuil H, Coimbra A, Triano P, et al. Ferumoxytol enhanced resting state fMRI and relative cerebral blood volume mapping in normal human brain. *Neuroimage*. 2013;83:200–209. [PubMed: 23831413]
48. Corot C, Robert P, Idee JM, Port M. Recent advances in iron oxide nanocrystal technology for medical imaging. *Advanced drug delivery reviews*. 2006;58(14):1471–1504. [PubMed: 17116343]
49. Aregger F, Wenaweser P, Hellige GJ, et al. Risk of acute kidney injury in patients with severe aortic valve stenosis undergoing transcatheter valve replacement. *Nephrology, dialysis, transplantation : official publication of the European Dialysis and Transplant Association - European Renal Association*. 2009;24(7):2175–2179. [PubMed: 19211648]
50. Bagur R, Webb JG, Nietlispach F, et al. Acute kidney injury following transcatheter aortic valve implantation: predictive factors, prognostic value, and comparison with surgical aortic valve replacement. *European heart journal*. 2010;31(7):865–874. [PubMed: 20037180]
51. Barbash IM, Ben-Dor I, Dvir D, et al. Incidence and predictors of acute kidney injury after transcatheter aortic valve replacement. *American heart journal*. 2012;163(6):1031–1036. [PubMed: 22709757]
52. Goebel N, Baumbach H, Ahad S, et al. Transcatheter aortic valve replacement: does kidney function affect outcome? *Ann Thorac Surg*. 2013;96(2):507–512. [PubMed: 23773729]
53. Sinning JM, Ghanem A, Steinhäuser H, et al. Renal function as predictor of mortality in patients after percutaneous transcatheter aortic valve implantation. *JACC Cardiovascular interventions*. 2010;3(11):1141–1149. [PubMed: 21087750]
54. Persson PB, Hansell P, Liss P. Pathophysiology of contrast medium-induced nephropathy. *Kidney international*. 2005;68(1):14–22. [PubMed: 15954892]
55. Yamamoto M, Hayashida K, Mouillet G, et al. Renal function-based contrast dosing predicts acute kidney injury following transcatheter aortic valve implantation. *JACC Cardiovascular interventions*. 2013;6(5):479–486. [PubMed: 23702012]

56. Powell AJ. SCMR Survey of Centers Performing CMR in Pediatric/Congenital Heart Disease. 2014.
57. Sorensen TS, Korperich H, Greil GF, et al. Operator-independent isotropic three-dimensional magnetic resonance imaging for morphology in congenital heart disease: a validation study. *Circulation*. 2004;110(2):163–169. [PubMed: 15210590]
58. Fenchel M, Greil GF, Martirosian P, et al. Three-dimensional morphological magnetic resonance imaging in infants and children with congenital heart disease. *Pediatr Radiol*. 2006;36(12):1265–1272. [PubMed: 17006655]
59. Seeger A, Fenchel MC, Greil GF, et al. Three-dimensional cine MRI in free-breathing infants and children with congenital heart disease. *Pediatr Radiol*. 2009;39(12):1333–1342. [PubMed: 19798494]
60. Cheng JY, Hanneman K, Zhang T, et al. Comprehensive motion-compensated highly accelerated 4D flow MRI with ferumoxytol enhancement for pediatric congenital heart disease. *J Magn Reson Imaging*. 2015.
61. Zhou Z, Han F, Rapacchi S, Ayad I, Salusky I, Plotnik A, Finn JP, Hu P. Accelerated Four-dimensional, multiphase, steady-state imaging with Contrast Enhancement (MUSIC) using Parallel Imaging and Compressed Sensing. In *Proceedings of the 23rd Annual Meeting of ISMRM*. Toronto, Ontario, Canada 2015. p. 180.
62. Han F, Zhou Z, Han ES, Finn JP, Hu P. Cardiac and respiratory self-gated 4D multi-phase steady-state imaging with ferumoxytol contrast (MUSIC). *Journal of Cardiovascular Magnetic Resonance*. 2016;18(Suppl 1):O51.
63. Hope MD, Hope TA, Zhu C, et al. Vascular Imaging With Ferumoxytol as a Contrast Agent. *AJR American journal of roentgenology*. 2015;205(3):W366–373. [PubMed: 26102308]
64. Corwin MT, Fananapazir G, Chaudhari AJ. MR Angiography of Renal Transplant Vasculature with Ferumoxytol:: Comparison of High-Resolution Steady-State and First-Pass Acquisitions. *Academic radiology*. 2015.
65. Florian A, Ludwig A, Rosch S, et al. Positive effect of intravenous iron-oxide administration on left ventricular remodelling in patients with acute ST-elevation myocardial infarction - A cardiovascular magnetic resonance (CMR) study. *International journal of cardiology*. 2014.
66. Yilmaz A, Dengler MA, van der Kuip H, et al. Imaging of myocardial infarction using ultrasmall superparamagnetic iron oxide nanoparticles: a human study using a multi-parametric cardiovascular magnetic resonance imaging approach. *European heart journal*. 2013;34(6):462–475. [PubMed: 23103659]

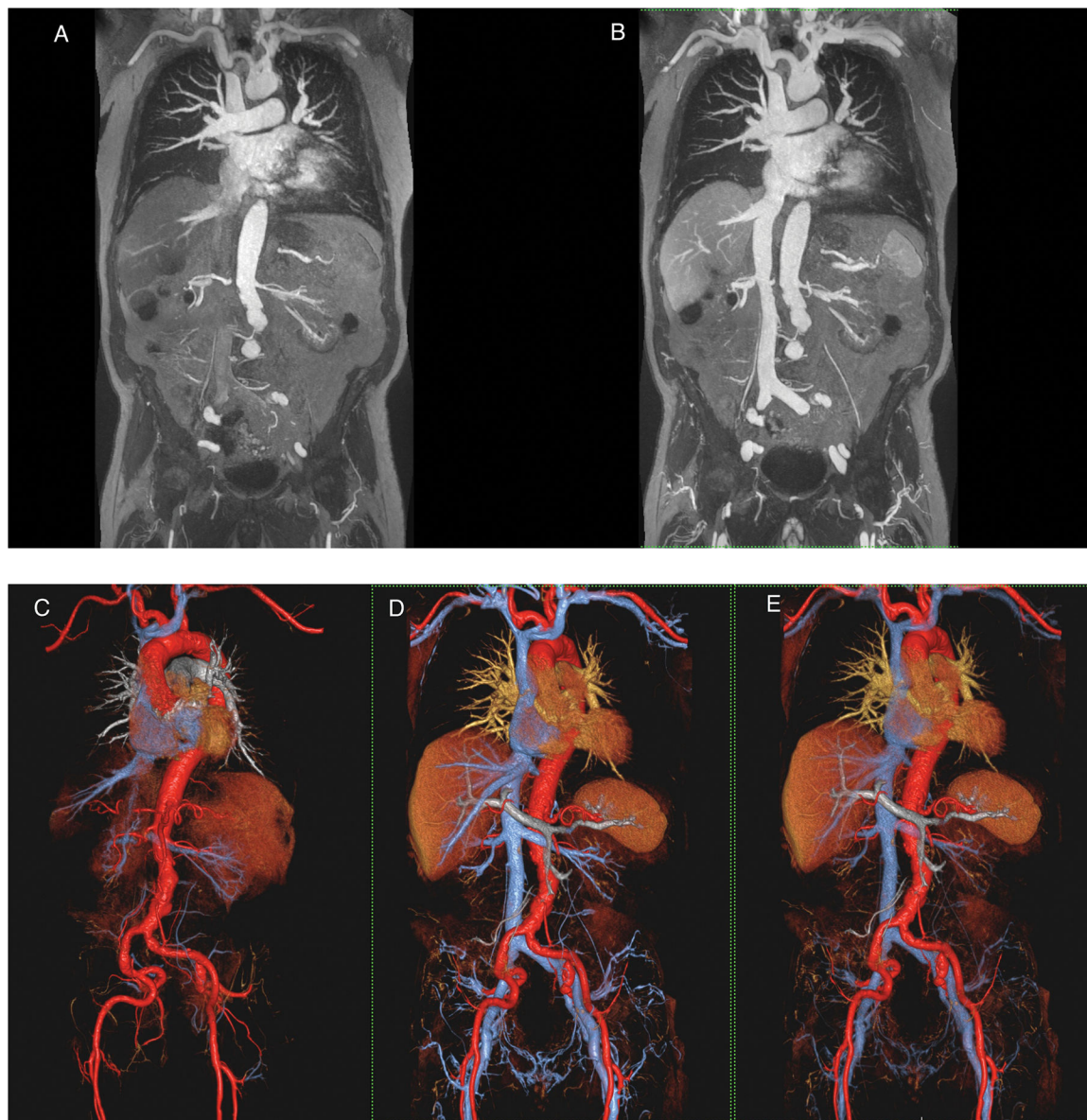
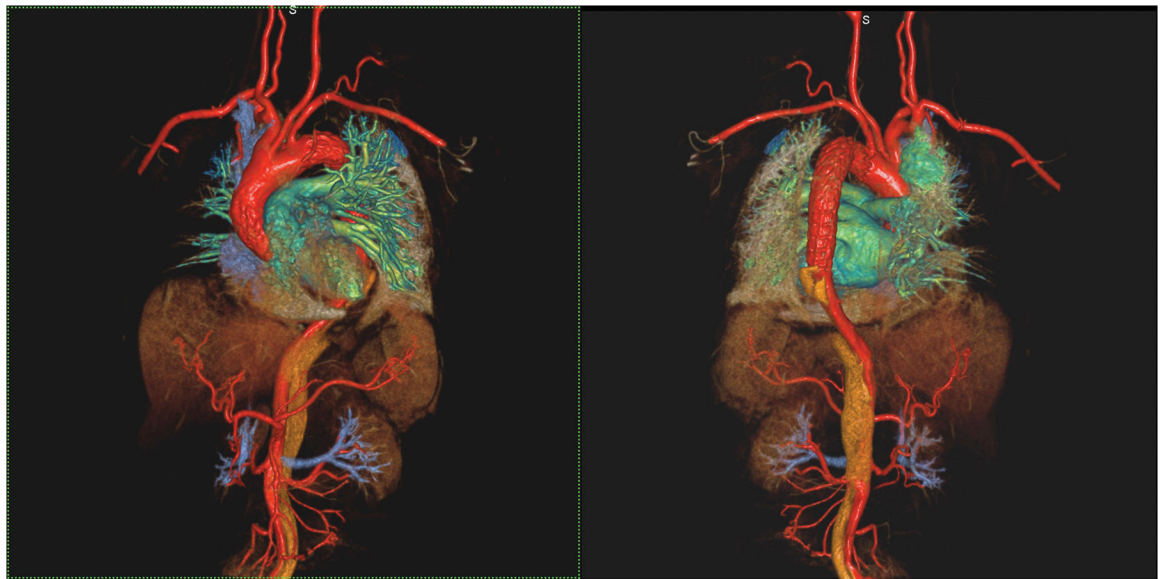
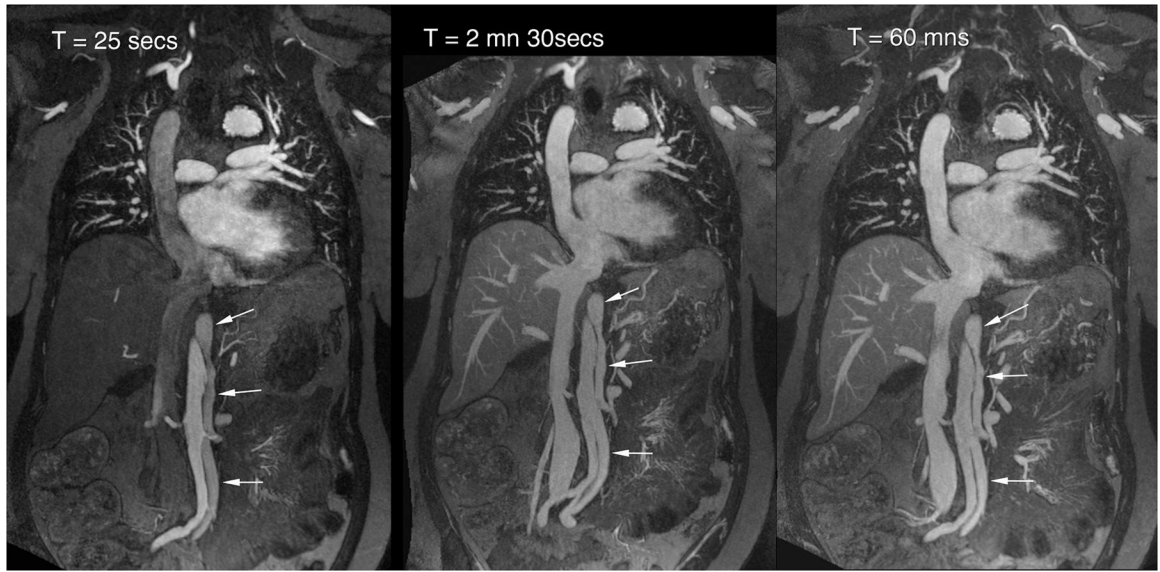


Figure1 (A-E).

A 90 year old male patient with renal failure undergoing vascular evaluation for transcatheter aortic valve replacement (TAVR). First pass imaging with ferumoxytol (A,C) on thin maximum intensity projection (MIP) (A) and volume rendered (VR) (C) reconstructions show similar bright and uniform arterial enhancement as on steady state images (B,D,E), where arteries and veins show equal signal intensity. In E, the systemic veins have been made more transparent. Note extensive irregularity and tortuosity in the aorto-iliac vessels. This study was acquired at 3.0T.



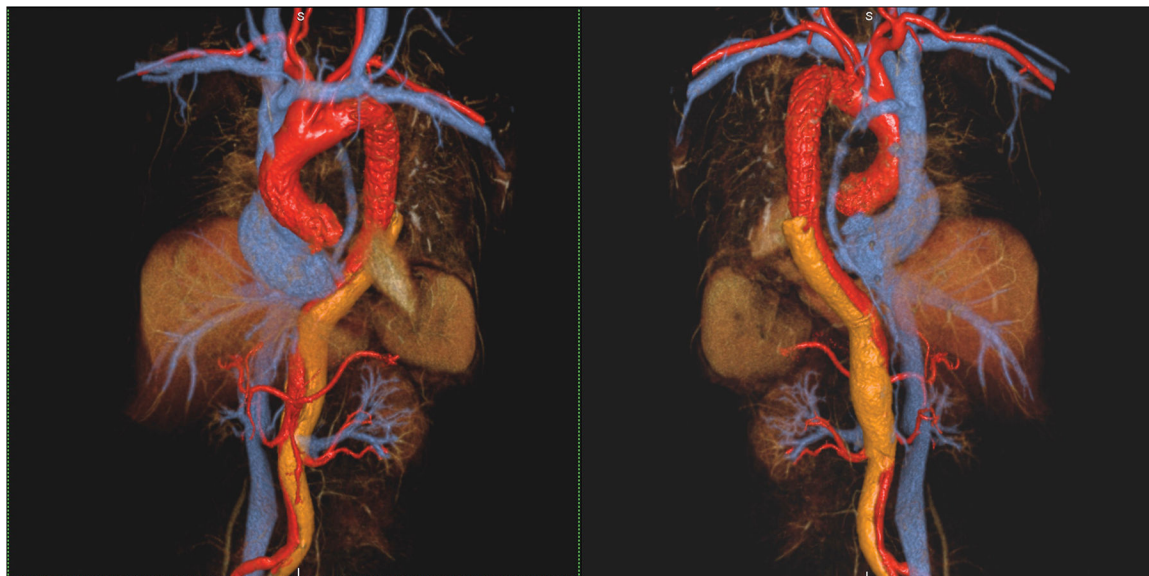


Figure 2 (A-C).

A 53 year old female with chronic, treated type A dissection and an endovascular thoracic aortic stent had ferumoxytol imaging because of severe renal impairment. Thin MIP images in A show the vascular enhancement status on first pass (left), two minutes post injection (middle) and one hour post injection. Differential enhancement of true and false (arrows) lumens is obvious on first pass, with uniform and stable enhancement of both lumens once the steady state is established. Volume rendered images of the first pass (B) and steady state (C) distribution phases show substantially similar anatomic information. Note the outline of the endovascular stent struts in the thoracic aorta. This study was acquired at 3.0T.

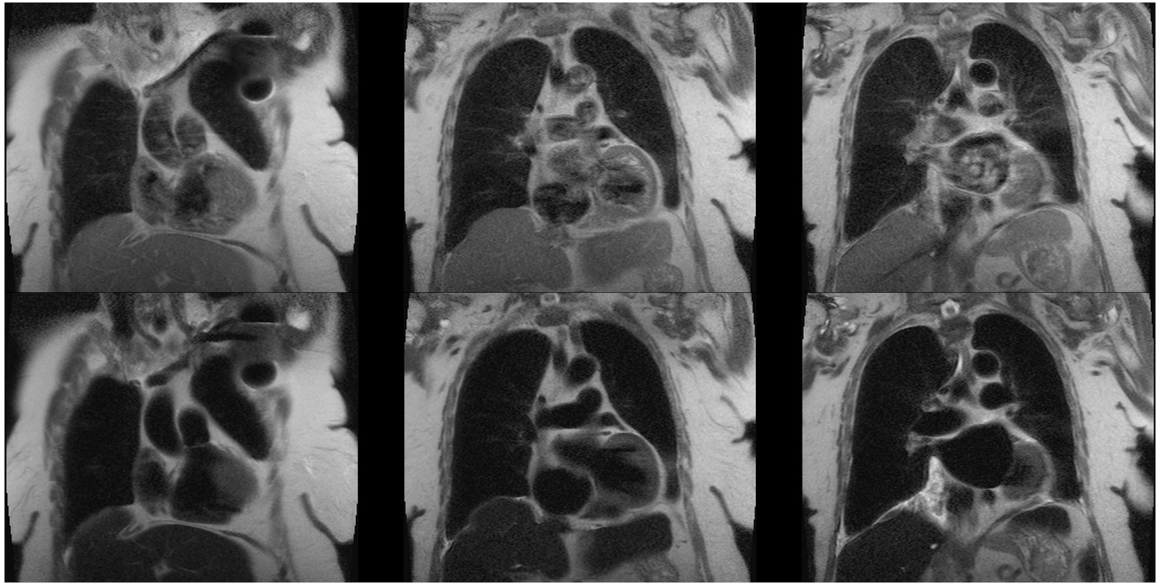


Figure 3.

A 64 year old female with a pacemaker and renal impairment undergoing evaluation for TAVR placement. Pre-contrast black blood HASTE images (top row) show extensive intravascular signal due to slow flow, despite double inversion pulses. Post-ferumoxytol HASTE images (bottom row) with exactly the same parameters show complete suppression of the intravascular and intracardiac blood signal. This study was acquired at 1.5T.

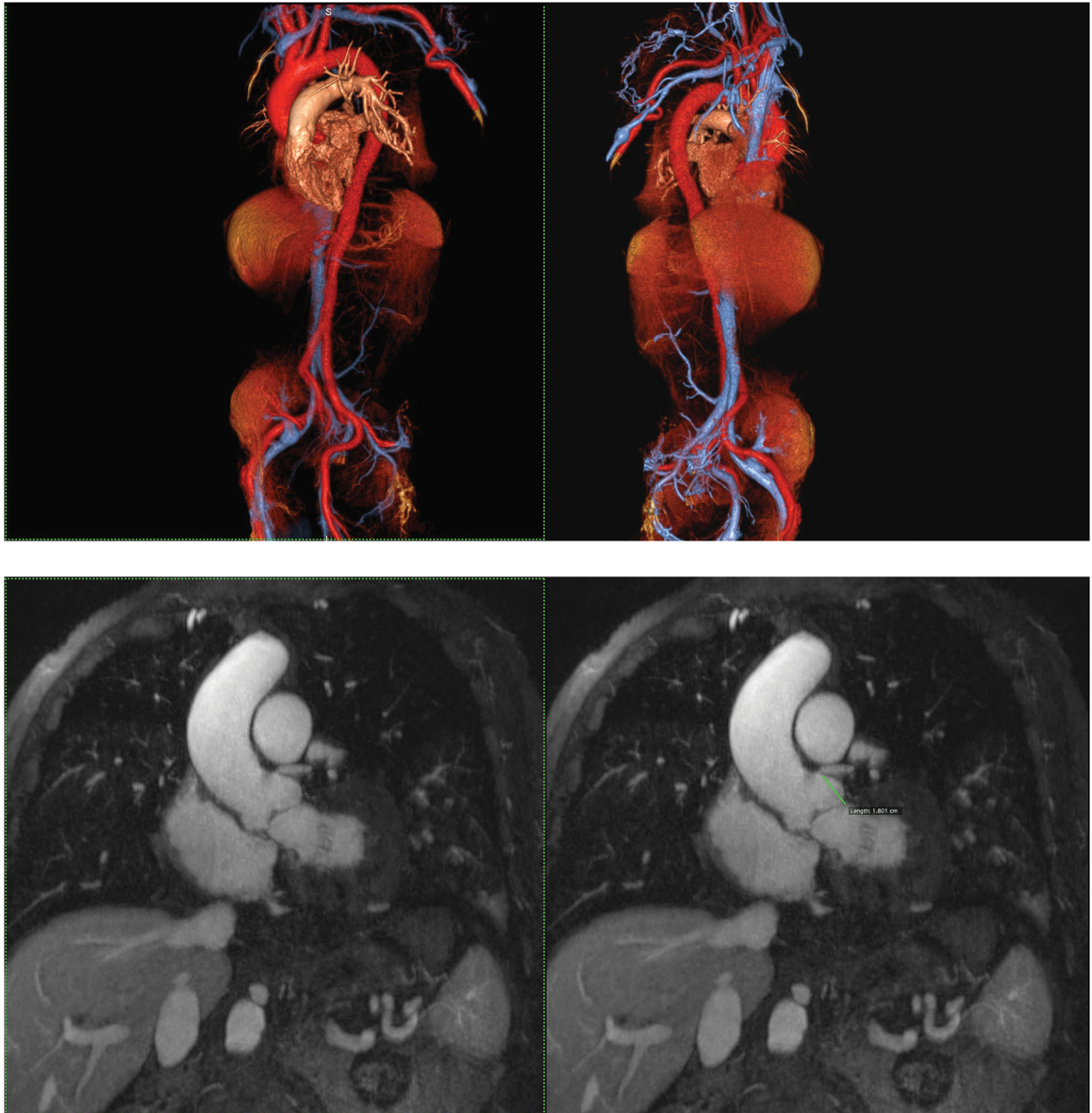


Figure 4 (A,B).

An 87 year old male with aortic stenosis, sinus bradycardia and renal transplant undergoing evaluation for TAVR placement. Volume rendered images in the steady state distribution of ferumoxytol (A) display the entire aorto-iliac anatomy as well as the patent renal transplant artery and vein in the pelvis. Gated, spoiled gradient echo cine images show the aortic valve leaflets and the relationship of the left coronary artery ostium to the annulus (B).

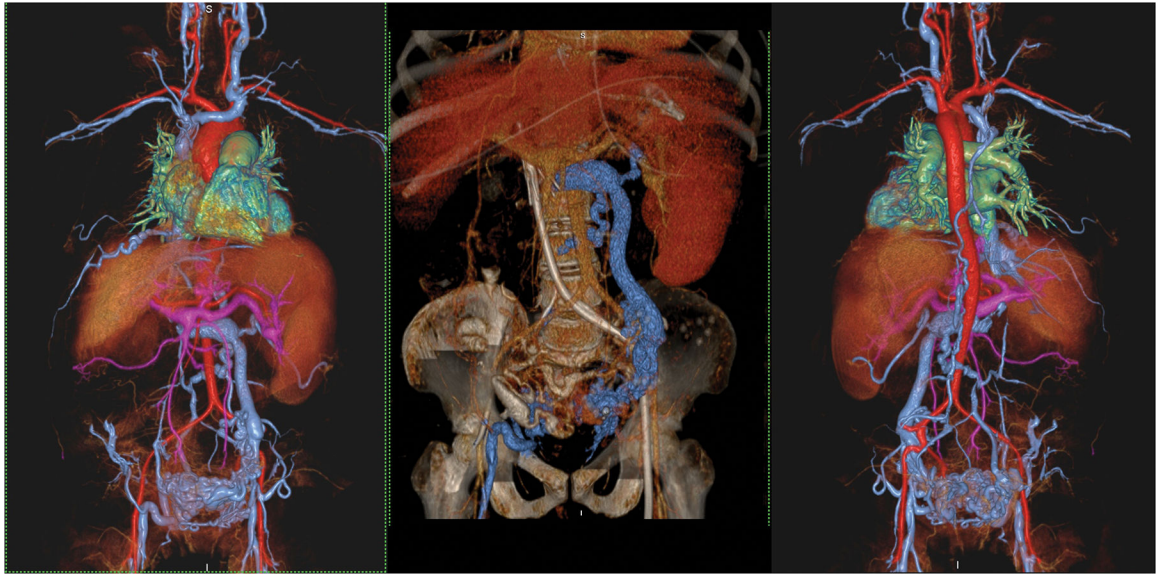
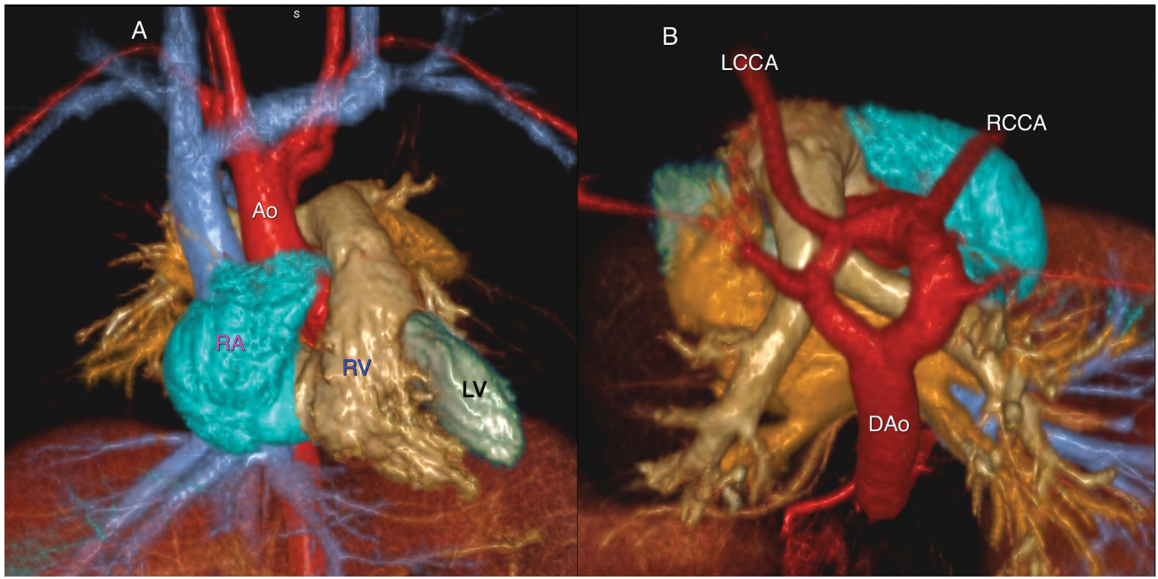


Figure 5.

A 46 year old female with end stage renal failure and liver disease with extensive venous thrombosis. Undergoing evaluation for organ transplantation. Volume rendered acquisition with steady state ferumoxytol (left and right frames) show detailed vascular anatomy of the thorax, abdomen and pelvis, including a hugely dilated left gonadal vein and pelvic varices. A CT venogram (middle frame) performed shortly prior to MRI suffers from contrast dilution with poorer vascular definition. Note the left sided venous catheter extending proximally through the occluded IVC. The MRI study was acquired at 3.0T.



Author Manuscript

Author Manuscript

Author Manuscript

Author Manuscript



Figure 6.

A 19 month old male with stridor and no prior history of congenital heart disease. Volume rendered reconstruction from a single frame of a 4-D MUSIC acquisition (6A) from the anterior (left frame) and superior (right frame) perspective show a complete vascular ring due to a double arch, with normal cardiac chamber anatomy.

Labels: RA right atrium; RV right ventricle; LV left ventricle, Ao ascending aorta; DAo descending aorta; LCCA left common carotid artery; RCCA right common carotid artery.

Dynamic evaluation of the 4D MUSIC data confirmed compression of the trachea, summarized in 6B. This study was acquired at 3.0T.

Table 1:

Technical Parameters

	First-pass FE-MRA	MUSIC	Self-gated MUSIC
Flip angle [degree]	20	20	
Bandwidth [Hz/pixel]	610	800	
TE/TR [ms]	1.0/2.7	1.1 / 3.0	
Field of view [mm]	500×300×150	500×300×150	
Resolution [mm]	1.0–1.2	0.8–1.0	
Cardiac phase number	-	6–9	9–18
Temporal Resolution [ms]	-	90–60	60–30
Accelerated acquisition	3X (GRAPPA and Partial Fourier)		6X (Compressed Sensing)
Scan Time [s]	22–30s	7–9 min	4–6 min
Respiratory motion compensation	Breath-held	Airway pressure	Self-gated
Cardiac motion compensation	None	ECG	Self-gated

Author Manuscript

Author Manuscript

Author Manuscript

Author Manuscript

Table 2.

Cardiovascular clinical studies using ferumoxytol as an MRI contrast agent

Author	Year	N	Age range	Clinical indications
Hope MD et al (63)	2015	102	70.7 ± 10.5 years	AAA, TAA, PE, aortic dissections, aneurysms, AVF, coronaries, carotids, LE vasculature
Cheng JY et al (60)	2015	23	6.3 (0 to 22.1) years	Congenital heart disease
Corwin MT et al (64)	2015	15	Mean 56.9 years	Renal transplant vascular patency
Walker JP et al (32)	2015	10	68 ± 4 years	Peripheral arterial disease
Ruangwattanapaisarn N et al (30)	2014	23	3 days – 18 years	Congenital heart disease
Han F et al (29)	2014	8	3 days – 5 years	Congenital heart disease
Nayak AB et al (28)	2014	10	4–18 years	CKD on hemodialysis – kidney transplant, biliary/liver dysfunction, vascular access
Florian A et al (65)	2014	17	56 ± 9 years	Myocardial infarct imaging (STEMI)
Bashir MR et al (43)	2014	17	62.8 ± 14.9 years	Abdominal pelvic and LE venography
Bashir MR et al (27)	2013	16	54 (36–73) years	Renal transplant vascular patency
Yilmaz A et al (66)	2012	14	51 (45–54) years	Myocardial infarct characterization (STEMI)
Alam SR et al (44)	2012	16	55 (48–65) years	Myocardial inflammation (STEMI)
Sigovan M et al (26)	2012	10	64 (59–82) years	Hemodialysis fistulas
Li W et al (25)	2005	11	64 (19–86) years	Vascular – carotids, thoracic and abdominal aorta, peripheral arteries

AAA abdominal aortic aneurysms, AVF arteriovenous fistulas, CKD chronic kidney disease, LE lower extremity, STEMI ST-elevation myocardial infarction, TAA thoraco-abdominal aneurysms,